Determination of the Thermal Lens in Solid-State Lasers with Stable Cavities

Beat Neuenschwander, Rudolf Weber, and Heinz P. Weber, *Fellow, IEEE*

Abstract— **A useful method to determine the thermal lens in a thermally loaded material inside a laser resonator under operation is presented. The laser beam emitted is focused with a lens placed exactly at the distance of its focal length behind the output mirror. For stable spherical resonators this focusing is not astigmatic even for an astigmatic cavity. This fact is used to experimentally determine the thermal lens including the beam quality factor (beam propagation factor) M^2 of the laser beam. Measurements are presented for an end-pumped rod and a longitudinally pumped slab laser serving as an example for an astigmatic cavity.**

I. Introduction

PUMPING of solid-state lasers leads to a spatial dependence of the temperature distribution in the laser crystal which is pronounced in the case of longitudinally diode pumping. Thermal dispersion, surface bending, as well as stress and strain lead therefore to a spatially varying refractive index imposing a nonuniform phase shift onto a beam passing through the crystal. This phase shift results in an optical beam distortion. To achieve a good spatial mode overlap between pump radiation and laser beam, necessary for high efficiencies, these effects have to be considered.

Uniform heating was extensively investigated for both, flash lamp pumping and transversal diode pumping [1], [2] and also for slab geometries [3]. Longitudinal pumping leads to the most pronounced non uniform heating resulting from the localized absorption of the pump radiation. Recent works [4]–[8] have used the axial symmetry of a rod and dealt with thermal beam distortion in edge and face cooled rod systems using analytical models or computer simulations. The thermal beam distortions were verified experimentally by interferometric methods [7], [8] or using a probe beam [2], [9]. In all cases, the phase shift profile was parabolic over the extent of the laser beam in the first order. Thus, the crystal is nearly acting as a spherical lens.

However, both methods mentioned above use a second laser either as probe beam or for the interferometer. In this paper, a simple method is presented which allows to determine the focal length of the thermal lens (which is assumed to be an ideal thin lens) in the crystal directly from the laser beam itself even for astigmatic resonators with a spherical output mirror. Near and far-field distributions of the laser output for pump powers up to 6 W have been recorded. The according beam radii were defined by the second moments [10] of these intensity distributions. From this the beam quality, factor M^2 was deduced which allowed to calculate the corresponding ideal thin thermal lens in the resonator. Measurements were carried out with a single end pumped rod and a single longitudinally pumped slab crystal [11]. The results for the such evaluated thermal lens for the rod were compared with the results from the analytical model presented in [4].

Manuscript received July 30, 1994; revised December 9, 1994. This work was supported in part by the Swiss Commission for the Encouragement of Scientific Research.

The authors are with the Institute of Applied Physics, Sidlerstrasse 5, 3012 Berne, Switzerland.

IEEE Log Number 9410766.

II. Theory

A. Beam Propagation Outside the Resonator

Pumped solid state laser materials suffer from thermal effects which can be treated in first order as spherical lens. If a Brewster window is placed inside the resonator, the perpendicular and parallel (usually horizontal and vertical) plane have to be treated separately. The output beam carries the information about the focal lengths of the thermal lens. This information can be extracted with a suitable experimental set-up. To calculate back into the resonator, the beam propagation outside the resonator has to be considered. This is preferentially done by starting at the output mirror. In the following, the calculation of the beam propagation and the determination of the thermal lens is first demonstrated for the fundamental mode.

In a stable spherical resonator, the radius of curvature of the phase front of the laser beam must match the radius of curvature of the mirror. Therefore, the radius of curvature of the beam is the same in the horizontal and the vertical plane at the output mirror even for an astigmatic resonator. The output mirror is assumed to act as an ideal thin lens for the beam passing through it. Therefore, the radius of curvature of the phase front right behind the mirror, R_{out} is still the same for both, the horizontal and vertical plane. For the fundamental mode, the laser beam can be described with two complex q-parameters [12], one for each plane. The beam parameters, $q_{M,(h,\nu)}$, right behind the output mirror are given by

$$\frac{1}{q_{M,(h,\nu)}} = \frac{1}{R_{\text{out}}} - i \cdot \frac{1}{\omega^2_{M,(h,\nu)}} \cdot \frac{\lambda}{\pi} \tag{1}$$

where $\omega_{M,(h,\nu)}$ are the beam radii on the mirror, which usually are different in an astigmatic cavity.

Assuming a lens with focal length f_1 being placed at a distance d_1 behind the output mirror. The q-parameters at this lens are given by $q_{1,(h,\nu)} = q_{M,(h,\nu)} + d_1$. These parameters are transformed by the lens and equal directly behind the lens

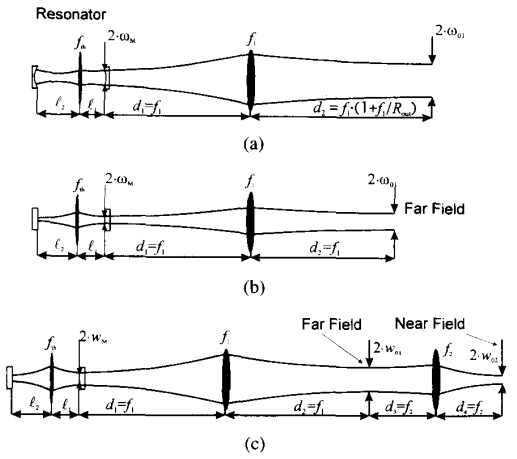

(a) (b) (c)

Fig. 1. Transformation of the output beam for a stable resonator containing the thermal lens f_{th}. The beam radius on the output mirror is $\omega_M(w_M)$. With the lens f_1 placed at the distance $d_1 = f_1$ behind the output mirror the new waist $\omega_{01}(w_{01})$ is located at the distance d_2. (a) With a spherical output mirror and fundamental mode operation. (b) With a plane output mirror and fundamental mode operation. The waist ω_{01} is also the location of the far field. (c) With a plane output mirror and multimode operation. The far field is located at the position of the waist w_{01}. In addition, the near-field lens f_2 placed at the distance $d_3 = f_2$ behind w_{01} defines the near-field distribution at $d_4 = f_2$ with the beam waist radius w_{02}. With w_{01}, w_{02}, and f_2, M^2 is obtained.

to [12]:

$$\frac{1}{q_{2,(h,\nu)}} = \frac{f_1 - (q_{M,(h,\nu)} + d_1)}{f_1 \cdot (q_{M,(h,\nu)} + d_1)}. \tag{2}$$

The lens f_1 produces new beam waists at the distances $d_{2,(h,\nu)} = \mathrm{Re}\,(q_{2,(h,\nu)})$. These distances depend on $q_{M,(h,\nu)}$ and are therefore usually different for the horizontal and the vertical plane for a astigmatic resonator, a fact which makes beam diagnostics rather troublesome. Fig. 1(a) shows the special situation if $d_1 = f_1$, i.e., if the lens is positioned at the distance of its focal length from the output mirror. The complex beam parameters $q_{2,(h,\nu)}$ reduces then to

$$q_{2,(h,\nu)} = -f_1 \cdot \left(1 + f_1 \cdot \frac{q^*_{M,(h,\nu)}}{|q_{M,(h,\nu)}|^2}\right) \tag{3}$$

where the asterisk terms the complex conjugated value. Taking into account, that $\mathrm{Re}\,(q^*_{M,(h,\nu)}/|q_{M,(h,\nu)}|^2) = \mathrm{Re}\,(1/q_{M,(h,\nu)})$, the distances $d_{2,(h,\nu)}$ are given by

$$d_{2,(h,\nu)} = -f_1 \cdot \left(1 + \frac{f_1}{R_{\mathrm{out}}}\right). \tag{4}$$

The negative sign in (4) means that the new waists are located on the opposite side of the lens than the output mirror. The distances $d_{2,(h,\nu)}$ of the waists only depend on the radius of curvature R_{out} and f_1. Therefore, the position of the waist is the same for both planes even for an astigmatic laser cavity, i.e., this focusing is not astigmatic.

The new waist radii, $\omega_{01,(h,\nu)}$ at this position can be calculated from $\mathrm{Im}\,(q_{2,(h,\nu)})$ and equal to

$$\omega_{01,(h,\nu)} = \frac{f_1}{\omega_{M,(h,\nu)}} \cdot \frac{\lambda}{\pi}. \tag{5}$$

Thus, with $d_1 = f_1$, the beam waits $\omega_{01,(h,\nu)}$ (the first subscript, 0, denotes a waist and the second, 1, refers to the lens f_1) can be measured at one single position. With that knowledge and (5), the beam radii $\omega_{M,(h,\nu)}$ on the output mirror can be calculated.

Fig. 1(b) shows the case of a plane output mirror. There (4) is reduced to $d_2 = -f_1$ and thus the far field is recorded. This is also valid for spherical output mirrors if $f_1 \ll R_{\mathrm{out}}$.

B. Ideal Thin Lens in a Plane–Plane Resonator

The knowledge of the beam radii on the output mirror allows to determine the focal length of a focusing element, i.e., a thermal lens $f_{th,(h,\nu)}$, inside the resonator. This is easy to understand in the case of a symmetric plane–plane resonator, where two beam waits exist, one on each mirror. Because the lens is placed exactly in the center of the resonator the radii of these two waists are identical. The radius of curvature of the phase front of the laser beam at both sides of the lens must therefore be equal and opposite. The radius is given by [12], [21]. With a resonator of length $l_{(h,\nu)}$ in this formula z is replaced by $l_{(h,\nu)}/2$. This radius of curvature is twice the focal length of a given lens causing this transformation. Therefore, the focal length $f_{th,(h,\nu)}$ of this lens can be expressed by the waist radius $\omega_{M,(h,\nu)}$ on the mirror:

$$f_{th,(h,\nu)} = \frac{(l_{(h,\nu)}/2)}{2} \cdot \left[1 + \left(\frac{\omega^2_{M,(h,\nu)} \cdot \pi}{(l_{(h,\nu)}/2) \cdot \lambda}\right)^2\right]. \tag{6}$$

Thus, with given far-field beam radii $\omega_{01,(h,\nu)}$, $\omega_{M,(h,\nu)}$ can be calculated with (5) as pointed out above and the focal lengths $f_{th,(h,\nu)}$ of a ideal thin lens inside the resonator can be determined for the horizontal and the vertical plane.

1) Special Situation: This straightforward thermal lens calculation can be applied also for end pumped rods. The situation that the input surface is the highly reflecting mirror and a plane output mirror is used can be transformed into the symmetric case mentioned above. This is done by mirroring the set-up at the input surface of the crystal. This symmetrized resonator is therefore twice as long i.e., in (6) $l_{(h,\nu)}/2$ has to be replaced by $l_{(h,\nu)}$. In this case, the beam passes through the thermal lens $f_{th,(h,\nu)}$ twice. This results in an effective thermal lens that is twice as strong as before, i.e., the focal length is halved. Therefore, the result of (6) must be doubled.

2) General Situation: A different calculation of $f_{th,(h,\nu)}$ has to be used if the crystal and, therefore, the thermal lens is not placed in the center of the resonator. In this case the assumption of the symmetry fails.

The focal length of the thermal lens $f_{th,(h,\nu)}$ is obtained by considering that the lens transforms the waist on the plane output mirror into a new waist on the (also plane) high reflecting mirror. Using [13, (1.70)], (6) has to be rewritten as (7) with $z_{0,(h,\nu)} = \omega^2_{M,(h,\nu)} \cdot \frac{\pi}{\lambda}$ found at the bottom of the next page.

In Fig. 1(b), the parameters of (7) are shown: $l_{1,(h,\nu)}$ is the distance between the output mirror and the thermal lens, $l_{2,(h,\nu)}$ is the distance between the lens and the high reflecting mirror and $\omega_{M,(h,\nu)}$ is obtained from the far field beam diameter $\omega_{01,(h,\nu)}$ and (5).

Usually a resonator containing a varying lens shows two stable zones as a function of the refractive power of the lens. The positive sign at the squareroot in (7) applies to the first stability zone, the negative sign to the second.

The conditions in the deviation of (6) and (7) are not fulfilled in the unstable zones. Therefore the calculation of the thermal lens as proposed in this section fails.

C. Ideal Thin Lens in a Resonator with Spherical Mirrors

Fig. 1(a) shows a resonator with spherical mirrors of finite radii. The determination of the focal length of the corresponding ideal thin lens becomes more difficult in this case. With a given lens inside the resonator the fundamental mode-beam radii on the output mirror are given by [13]:

$$\omega^2_{M,(h,\nu)} = \frac{\lambda \cdot L'_{(h,\nu)}}{\pi} \sqrt{\frac{g'_{2,(h,\nu)}}{g'_{1,(h,\nu)} \cdot (1 - g'_{1,(h,\nu)} \cdot g'_{2,(h,\nu)})}} \tag{8}$$

with the modified resonator lengths $L'_{(h,\nu)}$ and g-parameters $g'_{1,(h,\nu)}$ and $g'_{2,(h,\nu)}$:

$$L'_{(h,\nu)} = l_{1,(h,\nu)} + l_{2,(h,\nu)} - \frac{l_{1,(h,\nu)} \cdot l_{2,(h,\nu)}}{f_{th,(h,\nu)}}$$

$$g'_{1,(h,\nu)} = 1 - \frac{L'_{(h,\nu)}}{R_1} - \frac{l_{2,(h,\nu)}}{f_{th,(h,\nu)}} \tag{9}$$

$$g'_{2,(h,\nu)} = 1 - \frac{L'_{(h,\nu)}}{R_2} - \frac{l_{1,(h,\nu)}}{f_{th,(h,\nu)}}.$$

The radii of curvature are R_1 and R_2 for the output mirror and the high reflecting mirror, respectively. It is noted that formula (8) is identical with (6) in the symmetrical ($l_{1,(h,\nu)} = l_{2,(h,\nu)} = l_{(h,\nu)}/2$) plane–plane ($R_1 = R_2 = \infty$) case. Identical location of the horizontal and vertical waists (4) can also be achieved in the case of a spherical output mirror. It is reminded, that in (4) R_{out} is not the radius of curvature of the output mirror but the radius of curvature of the phase front of the laser beam directly behind the mirror. With the knowledge of $\omega_{M,(h,\nu)}$ on the mirror from $\omega_{01,(h,\nu)}$ with (5) the focal length $f_{th,(h,\nu)}$ of the lens can be determined iteratively.

D. Multimode Operation

The determination of the thermal lens $f_{th,(h,\nu)}$ as pointed out in the previous chapters is only valid for fundamental mode operation. In the following the considerations are expanded to the multimode situation. In this case, the beam radii and the half angle divergences are denoted by $w_{(h,\nu)}$ and $\Theta_{(h,\nu)}$ (Fig. 1(c)) instead of the fundamental mode notations $\omega_{(h,\nu)}$ and $\vartheta_{(h,\nu)}$, respectively. A formalism required to treat the multimode behavior in the same manner as the fundamental mode is the concept of the embedded fundamental mode [10], [14]. This embedded fundamental mode shows the same waist positions as the multimode beam, when it is transformed by optical elements and is therefore used to calculate backwards into the resonator. To define this embedded fundamental mode the beam quality factors (beam propagation factors) $M^2_{(h,\nu)}$ have to be determined. With the beam waist radii $w_{0,(h,\nu)}$ and the half angle divergences $\Theta_{(h,\nu)}$ they are given by

$$M^2_{(h,\nu)} = w_{0,(h,\nu)} \cdot \Theta_{(h,\nu)} \cdot \frac{\pi}{\lambda}. \tag{10}$$

This means that the multimode beam is $M^2_{(h,\nu)}$ times diffraction limited in the horizontal and the vertical plane. For this multimode beam, the beam waist radii $\omega_{0,(h,\nu)}$ and the half angle divergences $\vartheta_{(h,\nu)}$ of the embedded fundamental mode are then defined as [13]:

$$\omega_{0,(h,\nu)} = \frac{w_{0,(h,\nu)}}{M_{(h,\nu)}}, \vartheta_{(h,\nu)} = \frac{\Theta_{(h,\nu)}}{M_{(h,\nu)}}. \tag{11}$$

It is noted that for a fundamental mode $M^2_{(h,\nu)}$ exactly equals to one.

For treating a multimode beam not only the waist radii but also the half angle divergences of the beam have to be known. The set-up to deduce both is shown in Fig. 1(c). For a plane output mirror, the multimode beam has its waists directly on this mirror for both, the horizontal and the vertical plane. The radii are denoted by $w_{M,(h,\nu)}$. When the lens f_1 is positioned again at the distance of its focal length from the output mirror the new waists $w_{01,(h,\nu)}$ produced are located again at the distance $d_2 = f_1$. At this position, the far field is recorded as mentioned above. To deduce $M^2_{(h,\nu)}$, the half angle divergences $\Theta_{(h,\nu)}$ have to be measured. This is done using a second lens, the near-field lens, with focal length f_2. It is also placed at the distance of its focal length, $d_3 = f_2$, from the waists $w_{01,(h,\nu)}$. This lens again produces new waists, with radii $w_{02,(h,\nu)}$, at the distance $d_4 = f_2$ behind the lens. At this position, the near field is recorded. From the beam radii $w_{02,(h,\nu)}$ and f_2 the half angle divergences of the beam in front of the lens are given by $\Theta_{(h,\nu)} = w_{02,(h,\nu)}/f_2$ [13]. Taking (10) into account the beam quality factors $M^2_{(h,\nu)}$ therefore equals to:

$$M^2_{(h,\nu)} = \frac{w_{01,(h,\nu)} \cdot w_{02,(h,\nu)}}{f_2} \cdot \frac{\pi}{\lambda}. \tag{12}$$

Thus, with the knowledge of $w_{01,(h,\nu)}$ and $M^2_{(h,\nu)}$ the embedded fundamental mode is defined by (11). The waist radius of this embedded fundamental mode on the output mirror $\omega_{M,(h,\nu)}$ can then be calculated with (5).

This embedded fundamental mode is assumed to match the fundamental mode of the resonator. Therefore, the thermal lens in the resonator can be determined as pointed out in the

$$f_{th,(h,\nu)} = \frac{(l_{1,(h,\nu)} \cdot (l_{1,(h,\nu)} + 2 \cdot l_{2,(h,\nu)}) + z^2_{0,(h,\nu)}) \pm \sqrt{(l^2_{1,(h,\nu)} + z^2_{0,(h,\nu)})^2 - 4 \cdot l^2_{2,(h,\nu)} \cdot z^2_{0,(h,\nu)}}}{2 \cdot (l_{1,(h,\nu)} + l_{2,(h,\nu)})} \tag{7}$$

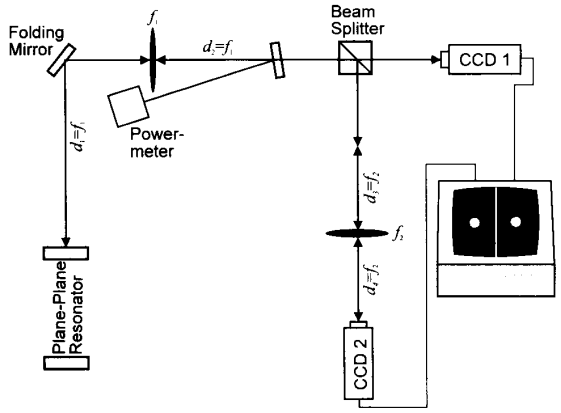

Fig. 2. The beam diagnostics set-up. The far- and the near-field intensity distribution were recorded by CCD cameras. The corresponding beam radii w_{01} and w_{02} were determined by the second moment method.

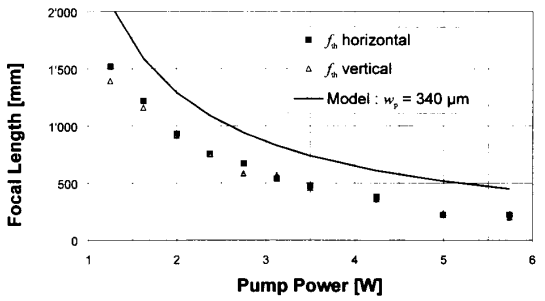

Fig. 3. The focal length f_{th} of the thermal lens versus incident pump power for the single end pumped rod. For the model a pump spot radius $w_p = 340$ μm was used.

previous chapters. This assumption is exactly fulfilled for resonators that contain ideal spherical elements. However, it can also be used as a good approximation for resonators containing elements introducing small deviations from a parabolic phase shift over the extension of the beam (e.g., real thermal lenses).

III. Experimental Setup

The setup for the beam diagnostics is shown in Fig. 2 and is equivalent to the situation shown in Fig. 1(b). To obtain a far field beam diameter of about 1 mm a far-field lens with a focal length of $f_1 = 510$ mm was used. The focal length of the near-field lens was $f_2 = 408$ mm. A folding mirror, without influence onto the beam, was used to compact the set-up. After passing through the far-field lens, the main part of the beam was reflected by a slightly tilted high reflecting mirror that allowed to measure the laser output power. After passing through the tilted mirror, the beam was divided into two parts by a beam splitter. One part of the beam was used to determine the far-field radii $w_{01,(h,\nu)}$ from the CCD1 record. The other part was directed through the near-field lens f_2 forming the near field on CCD2. From this the beam waist radii $w_{02,(h,\nu)}$ were determined using the second moment method described in [10]. Two monochrome CCD-cameras with a pixel size of 11.8 μm$*$ 8.3 μm have been used. The CCD-image was captured with an 8-bit frame-grabber and post-processed on a PC.

IV. Results

A. End-Pumped Rod

A single end pumped Nd:YAG rod with a length of 20 mm and a radius of 4.8 mm was used to check this technique for determining the thermal lens. In this case, the pumped surface of the rod was dichroically coated, highly reflecting for the laser wavelength of 1.06 μm and highly transmitting for the pump wavelength of 809 nm. The other surface was anti-reflection coated for 1.06 μm. As pump source a Jenoptik 10-W diode laser was used. It's output radiation was passed through a line-to-bundle fiber converter [15], [16] and coupled into a 600-μm multimode fiber with N.A. = 0.22. The fiber output was imaged by a two-lens optics onto the crystal surface. With this a pump spot radius in the crystal of 340 μm was achieved. The half angle divergence of the pump beam was 12.5°. The transfer efficiency from the diode laser to the crystal was about 55%. The resonator was formed by the pumped surface of the rod and a 5% output coupling mirror. The length of the resonator was 112 mm.

Fig. 3 shows the deduced thermal lens for the single end pumped rod in the horizontal and vertical plane as a function of the pump power. The pump power dependence of the measured focal length is nearly the same in the horizontal and the vertical plane as expected from to the radial symmetry of the cylindrical rod. The solid line is the result of an analytical model [4] which predicts a hyperbolic dependence of the thermal lens focal length from the pump power. All focal lengths are about 30% smaller than the theoretically predicted values.

This difference can be explained by the following facts: The model only takes into account the temperature induced change of the refractive index due to the thermal dispersion $\partial n/\partial T$. Not included in the analysis are the bending of the pumped surface and the stress and strain induced change of the refractive index. In the investigated pump power range, the surface bending is of importance and additionally reduces the focal length of the thermal lens by about 20% to 30% [8]. Moreover, the model dealt with a gaussian distributed pump radiation without divergence. In our case, the divergence of the pump beam is 12.5° with a changing distribution along the pump axis. Considering these effects, the analytical model and the measurements are in a very good agreement.

The beam quality factor M^2 as deduced from the waist measurements is shown in Fig. 4 as a function of pump power. Its value does never exceed 1.1, i.e., the laser was running nearly in a TEM_{00} mode.

With this arrangement a maximum output power of 2.7 W at a pump power of 5.7 W was achieved at a slope efficiency of 54%.

B. Single Longitudinally Pumped Slab

An astigmatic laser cavity was set up as presented in [11], but only single longitudinally pumped at one position. The

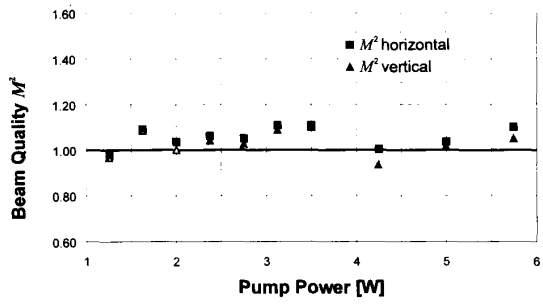

Fig. 4. Beam quality M^2 versus incident pump power for the single end-pumped rod.

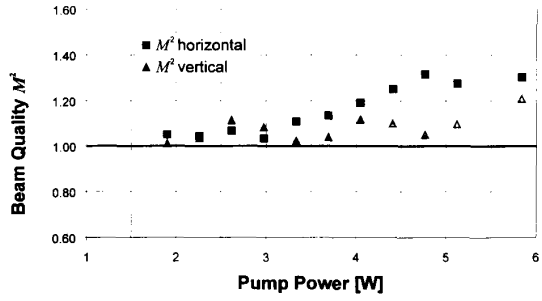

Fig. 6. Beam quality M^2 versus incident pump power for the single longitudinally pumped slab.

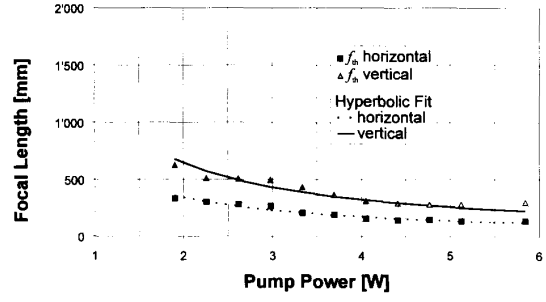

Fig. 5. The focal length f_{th} of the thermal lens versus the incident pump power for the single longitudinally pumped slab ($w_p = 340$ μm).

bottom and top surface of the crystal were in contact with a water cooled heat sink at room temperature. The output mirror was placed at a distance of 90 mm, the high reflecting mirror at a distance of 74 mm from the crystal. With a geometrical path length of the laser beam in the crystal of about 75 mm the effective resonator lengths became therefore 176.4 mm in the horizontal plane and 205 mm in the vertical plane due to the Brewster's surfaces of the crystal [17, 18].

For the single-pumped slab geometry, the deduced thermal lens as a function of pump power is shown in Fig. 5. The lines represent a hyperbolic fit to the data. The focal length is as in the previous example dependent of the inverse pump power. The thermal lens in the vertical plane is about the same as in the rod whereas it is almost twice as strong in the horizontal plane. This difference between the two planes is caused by the geometry of the crystal and the oblique incidence of the pump beam, a fact which is under investigation.

Fig. 6 shows the $M^2_{(h,\nu)}$ values for both planes in the slab. The beam quality increases with the pump power from 1 to 1.4 in the horizontal and from 1 to 1.3 in the vertical plane, respectively.

C. Error Discussion

The determination of the beam radii with the second moment of the intensity distribution is very sensitive to structures in the wings of the beam. Inaccuracies arise when records of beams containing such wings are post processed due to the noise of the CCD camera. The CCD-cameras used had an effective dynamic range of about 40. With this dynamic range the accuracy of the beam radii was found to be about $\pm 5\%$ for smooth beams. For beams with significant structures in the wings this accuracy was reduced up to about $\pm 20\%$. The lens and cameras have been positioned with an accuracy better than ± 1 mm and the accuracy of the focal lengths of the lenses are specified by the manufacturer to be better than $\pm 2\%$. Therefore, the error in the determination of $f_{th,(h,\nu)}$ and $M^2_{(h,\nu)}$ is mainly caused by the experimental uncertainties introduced by the determination of the beam radii. The accuracy of the second moment method can be increased considerably by the use of high dynamic range cameras.

With these experimental uncertainties the error in determining the thermal lens $f_{th,(h,\nu)}$ becomes about $\pm 16\%$ for smooth beams and up to $\pm 60\%$ for structured beams. For the beam quality factor $M^2_{(h,\nu)}$ the error amounts to about $\pm 7\%$ for smooth beams and up to $\pm 30\%$ in the worst case.

As previously mentioned, the embedded fundamental mode does not match exactly the fundamental mode defined by the resonator. This error was not included in the discussion above. It depends on the exact mode spectrum and is not straightforward to treat. Attempts in this direction will be subject of future investigations.

V. Conclusion

In this paper, a design to determine the focal length of a thermal lens inside a resonator without any probe beam was presented. This is accomplished directly from the out coming laser beam by simultaneously taking one picture of the intensity distribution in the far and near field with a CCD camera. Simultaneously this design allows to deduce the beam quality factor. This method is applicable for stable resonators with a spherical output mirror even in the case of astigmatic cavities.

With this set-up, the beam quality factor and the thermal lens have been determined for an end pumped rod and a single longitudinally pumped slab. Significantly different focal lengths of the thermal lens resulted in the two specific planes of the astigmatic slab cavity. The thermal lens for the end pumped rod was compared with an analytical model. The good agreement confirms the applicability of the presented set-up.

ACKNOWLEDGMENT

The authors thank P. Laedrach for his help with the post-processing program on the PC.

REFERENCES

[1] W. Koechner, *Solid-State Laser Engineering*, 3rd. ed. Berlin: Springer Verlag, 1992.
[2] J. E. Murray, "Pulsed gain and thermal lensing of Nd:$LiYF_4$," *IEEE J. Quantum Electron.*, vol. QE-19, no. 4, 488–491, 1983.
[3] J. M. Eggleston, T. J. Kane, K. Kuhn, J. Unternahrer, and R. L. Byer, "The slab geometry laser—Part I: Theory," *IEEE J. Quantum Electron.*, vol. QE-20, no. 3, pp. 289–301, 1984.
[4] M. E. Innocenzi, H. T. Yura, C. L. Fincher, and R. A. Fields, "Thermal modeling of continuous-wave end-pumped solid-state lasers," *Appl. Phys. Lett.*, vol. 56, no. 19, pp. 1831–1833, 1990.
[5] J. Frauchiger, P. Albers, and H. P. Weber, "Modeling of thermal lensing and higher order ring mode oscillation in end-pumped CW Nd:YAG lasers, " *IEEE J. Quantum Electron*, vol. 28, no. 4, pp. 1046–1056, 1991.
[6] A. K. Cousins, "Temperature and thermal stress scaling in finite-length end-pumped laser rods," *IEEE J. Quantum Electron.*, vol. 28, no. 4, pp. 1057–1069, 1991.
[7] S. C. Tidwell, J. F. Seamans, M. S. Bowers, and A. K. Cousins, "Scaling CW diode-end-pumped Nd:YAG lasers to high average powers," *IEEE J. Quantum Electron.*, vol. 28, no. 4, pp. 997–1009, 1992.
[8] C. Pfistner, R. Weber, and H. P. Weber, "Thermal beam distortion in longitudinally pumped solid-state lasers," *IEEE J. Quantum Electron.*, vol. 30, no. 7, pp. 1605–1616, 1994.
[9] G. Cerullo, S. De Silvestri, and V. Magni, "High efficiency 40 W Nd:YLF laser with large TEM_{00} mode," *Opt. Commun.*, vol. 93, no. 1, 2, pp. 77–81, 1992.
[10] P. A. Belanger, "Beam propagation and the ABCD ray matrices," *Opt. Lett.*, vol. 16, no. 4, pp. 196–199, 1991.
[11] B. Neuenschwander, P. Albers, and H. P. Weber, "Efficient multiple-longitudinally diode laser pumped Nd:YAG slab laser," *Opt. Quantum. Electron.*, vol. 24, no. 3, pp. 363–370, 1992.
[12] H. Kogelnik and T. Li, "Laser beams and resonators," *Appl. Opt.*, vol. 5, no. 10, pp. 1550–1567, 1966.
[13] N. Hodgson and H. Weber, *Optische Resonatoren.* Berlin: Springer Verlag, 1992.
[14] T. F. Johnston, Jr., "M^2 concept characterizes beam quality," *Laser Focus World*, vol. 26, pp. 173–183, 1990.
[15] H. Zbinden and J. E. Balmer, "Q-switched Nd:YLF laser end pumped by a diode-laser bar," *Opt. Lett.*, vol. 15, no. 18, pp. 1014–1016, 1990.
[16] TH. Graf. and J. E. Balmer, "High-power Nd:YLF laser end pumped by a diode-laser bar," *Opt. Lett.*, vol. 18, no. 16, pp. 1317–1319, 1993.
[17] H. W. Kogelnik, E. P. Ippen, A. Dienes, and C. V. Shank, "Astigmatically compensated cavities for CW dye lasers," *IEEE J. Quantum Electron*, vol. QE-8, no. 3, pp. 373–379, 1972.
[18] D. C. Hanna, "Astigmatic Gaussian beams produced by axially asymmetric laser cavities," *IEEE J. Quantum Electron.*, vol. QE-5, no. 10, pp. 483–488, 1969.

Beat Neuenschwander was born in Switzerland, in Decembre 28, 1964. He received the Diploma in physics from the University of Berne, Switzerland, in 1992 and is currently working towards the Ph.D. degree at the Institute of Applied Physics, Berne, Switzerland.

He has been engaged in research on diode pumped solid state lasers. His present research interests include thermal effects in diode pumped solid state laser crystals.

Rudolf Weber was born 1957 in Biel, Switzerland. He studied physics at the University of Berne, where he received the physics diploma and the Ph.D. degree, both on the field of laser produced plasma.

He is project leader of a laser surface interaction and diode pumped solid-state laser project.

Heinz P. Weber (M'72–SM'85–F'89) received the Diploma in Physics from the ETH Zuerich, Switzerland in 1964 and the Ph.D. degree from the University of Berne, Switzerland in 1968.

His thesis was on generation and measurements of ps lightpulses, his main contribution was the discovery of the intensity correlation method for timeduration measurement. In 1969 he joined Bell Laboratories, Holmdel, USA, where he was involved in research on integrated optics and also in investigations of rare-earth laser crystals with a high Nd concentration. In 1975, he became Professor and head of the laser departement of the Institute of Applied Physics at the University of Berne, Switzerland, and is presently interested in mode-locking and nonlinear effects in propagation of lightpulses through optical fibres, solid-state lasers and laser surgery.

Dr. Weber is member of the "Swiss Academy of Technical Sciences" and a fellow of the Optical Society of America. Presently, he serves as board member of of the Swiss Society for Optics and Electron Microscopy.